Electronic Supplementary Information

Two ways spin crossover in iron(II) coordination polymer associated with conformational changes of bridging ligand

Maria Książek,[a] Marek Weselski,[b] Agnieszka Dreczko,[b] Vladyslav Maliuzhenko,[b] Marcin Kaźmierczak,[b] Aleksandra Tołoczko,[b] Joachim Kusz,[a] Robert Bronisz[b]*

[a] *Institute of Physics, University of Silesia, 75 Pułku Piechoty 1, 41-500 Chorzów, Poland.*
[b] *Faculty of Chemistry, University of Wrocław, F. Joliot-Curie 14, 50-383, Wrocław, Poland.*

Contents:

Table S1. Crystallographic data for **bbtre** (CCDC 1885384) at 290 K.

Chemical formula	$C_{12}H_{20}N_6$
Formula Mass	248.34
Crystal system	Monoclinic
Space group	P 2_1/c
Z	2
Unit cell dimensions *a*/Å *b*/Å *c*/Å *α*/° *β*/° *γ*/°	 7.9659(12) 10.0866(13) 8.5204(19) 90 91.881(15) 90
Unit cell volume/Å^3	684.2(2)
F(000)	268
D_x (Mg m^{-3})	1.205
μ (mm^{-1})	0.078
Theta range for data collection/°	3.995 to 26.372
Range of *h*, *k*, *l*	-9 ≤ *h* ≤ 9 -12 ≤ *k* ≤ 12 -5 ≤ *l* ≤ 10
No. of measured reflections	5415
No. of independent reflections	1399
R_{int}	0.0228
Data / restraints / parameters	1399 / 0 / 103
Goodness-of-fit on F^2	1.138
Final R_1 values ($I > 2\sigma(I)$)	0.0765
Final $wR(F^2)$ values ($I > 2\sigma(I)$)	0.2590
Final R_1 values (all data)	0.0849
Final $wR(F^2)$ values (all data)	0.2661
Largest diff. peak and hole/eÅ^3	0.206 and -0.222

Table S2. Crystallographic data for complex **1** at various temperatures.

	HT(HS)	**LT(HS)**	**LT(HS/LS)**	**HT1(LS)**	**HT1(HS)**	**HT2(HS)** (average structure)	**HT2(LS)** (average structure)
CCDC number	**1953184**	**1953185**	**1953186**	**1953187**	**1953188**	**1953189**	**1953190**
T/K	295 K	200 K	80 K	80 K	150 K	170 K	80 K
Chemical formula	$C_{40}H_{66}FeN_{20}Cl_2O_8$	$C_{40}H_{66}FeN_{20}Cl_2O_8$	$C_{40}H_{66}FeN_{20}Cl_2O_8$	$C_{40}H_{66}FeN_{20}Cl_2O_8$	$C_{40}H_{66}FeN_{20}Cl_2O_8$	$C_{40}H_{66}FeN_{20}Cl_2O_8$	$C_{40}H_{66}FeN_{20}Cl_2O_8$
Formula Mass	1081.87	1081.87	1081.87	1081.87	1081.87	1081.87	1081.87
Crystal system	Triclinic						
Space group	P-1	P-1	P-1	P-1	P-1	P-1	P-1
Z	1	2	2	1	1	1	1
Unit cell dimensions							
a/Å	10.7647(12)	12.6332(5)	12.5034(4)	10.6081(4)	10.5814(9)	10.5853(3)	10.4994(2)
b/Å	12.3715(19)	12.6307(5)	12.4324(4)	12.2651(5)	12.2474(11)	12.3116(4)	12.2450(4)
c/Å	12.6339(12)	20.0943(8)	19.9466(6)	12.2885(5)	12.3911(10)	12.3848(3)	12.1324(3)
α/°	80.904(11)	76.144(4)	76.225(3)	82.533(3)	84.459(7)	84.833(2)	84.628(2)
β/°	71.656(10)	75.831(4)	75.945(3)	72.690(4)	74.221(7)	74.339(2)	73.4236(19)
γ/°	72.218(12)	83.005(3)	83.381(3)	72.256(4)	73.784(8)	73.659(3)	72.557(2)
Unit cell volume/Å^3	1517.2(3)	3011.6(2)	2915.88(17)	1452.46(11)	1483.5(2)	1491.15(7)	1426.18(6)
F(000)	570	1140	1140	570	570	570	570
D_x (Mg m^{-3})	1.184	1.193	1.232	1.237	1.211	1.205	1.260
μ (mm^{-1})	0.395	3.321	3.430	0.413	3.371	0.402	0.421
Theta range for data collection/°	3.250 to 26.372	3.612 to 73.408	3.651 to 73.878	3.066 to 35.934	3.708 to 73.576	3.191 to 26.372	3.244 to 26.370
Completeness	theta = 25.242° 89.9	theta = 67.684° 99.7 %	theta = 67.684° 99.4 %	theta = 25.500° 99.9 %	theta = 67.684° 99.9 %	theta = 25.242° 99.7 %	theta = 25.242° 99.8 %
Range of *h*, *k*, *l*	-13 ≤ *h* ≤ 8 -15 ≤ *k* ≤ 15 -11 ≤ *l* ≤ 14	-15 ≤ *h* ≤ 15 -15 ≤ *k* ≤ 14 -19 ≤ *l* ≤ 24	-15 ≤ *h* ≤ 15 -15 ≤ *k* ≤ 14 -20 ≤ *l* ≤ 24	-17 ≤ *h* ≤ 14 -20 ≤ *k* ≤ 17 -19 ≤ *l* ≤ 20	-13 ≤ *h* ≤ 11 -15 ≤ *k* ≤ 13 -15 ≤ *l* ≤ 15	-10 ≤ *h* ≤ 13 -15 ≤ *k* ≤ 15 -15 ≤ *l* ≤ 15	-11 ≤ *h* ≤ 13 -15 ≤ *k* ≤ 15 -15 ≤ *l* ≤ 15
No. of measured reflections	5943	20643	20297	21201	10551	12419	11877
No. of independent reflections	5472	11737	11299	12339	5779	6093	5813
R_{int}	0.0184	0.0898	0.0391	0.0251	0.0790	0.0243	0.0230
Data / restraints / parameters	5472 / 103 / 375	11737 / 92 / 788	11299 / 97 / 786	12339 / 134 / 443	5779 / 126 / 442	6093 / 239 / 431	5813 / 130 / 422
Goodness-of-fit on F^2	1.301	1.277	1.295	1.217	1.087	1.419	1.606
Final R_1 values ($I > 2\sigma(I)$)	0.1359	0.1165	0.1075	0.0865	0.1090	0.1018	0.1064
Final $wR(F^2)$ values ($I > 2\sigma(I)$)	0.3564	0.3002	0.3032	0.2439	0.2838	0.3040	0.3319
Final R_1 values (all data)	0.1861	0.1381	0.1360	0.1065	0.1334	0.1123	0.1148
Final $wR(F^2)$ values (all data)	0.4091	0.3295	0.3362	0.2656	0.3180	0.3227	0.3481
Largest diff. peak and hole/eÅ^3	1.080 and -1.104	1.179 and -1.013	1.059 and -0.910	1.202 and -0.829	0.962 and -0.943	1.484 and -1.034	1.793 and -1.143

Table S3. Selected Fe-N distances (Å), torsion angles (°) and Fe···Fe interatomic distances (Å) for HT(HS) at 295 K in **1**. *t = trans, g = gauche*.

	295 K (cooling) HT(HS)
Fe1-N1A	2.201(5)
Fe1-N1B	2.162(5)
Fe1-N1C	2.167(5)
Fe1···Fe1^{i} [-110] (***ttt***)	13.696(2)
C1c-C3c-C4c-C4c^{ii}	179(1) (***t***)
C3c-C4c-C4c^{ii}-C3c^{ii}	180 (***t***)
Fe1···Fe1^{iii} [10-1] (***ttt***)	13.780(2)
C1b-C3b-C4b-C4b^{iv}	174(2) (***t***)
C3b-C4b-C4b^{iv}-C3b^{iv}	180 (***t***)
Fe1···Fe1^{v} [001] (***gtg***)	12.634(1)
C1a-C3a-C4a-C4a^{vi}	-64(1) (***g***)
C3a-C4a-C4a^{vi}-C3a^{vi}	180 (***t***)

Symmetry operations: ^{i} 1+x, -1+y, z; ^{ii} 2-x, -y, 1-z; ^{iii} -1+x, y, 1+z; ^{iv} –x, 1-y, 2-z; ^{v} x, y, -1+z; ^{vi} 1-x, 1-y, -z

Table S4. Selected Fe-N distances (Å), torsion angles (º) and Fe···Fe interatomic distances (Å) for LT(HS) at 200 K (cooling) and for LT(LS) at 80 K in **1**. ***t*** *= trans,* ***g*** *= gauche*.

	200 K (cooling) LT(HS)	**80 K (cooling) LT(HS)**
Fe1-N3	2.201(4)	2.144(5)
Fe1-N13	2.195(4)	2.138(5)
Fe1-N23	2.192(4)	2.130(4)
Fe1-N33	2.200(4)	2.136(4)
Fe1-N43	2.204(4)	2.144(5)
Fe1-N53	2.207(4)	2.148(4)
Fe1···Fe1^{i} [1-1-1]* (***ttt***)	13.728(1)	13.608(2)
C21-C23-C24-C24^{i}	179.4(7) (***t***)	179.9(8) (***t***)
C23-C24-C24^{i}-C23^{i}	180 (***t***)	180 (***t***)
Fe1···Fe1^{ii} [1-1-1]* (***gtg***)	12.602(1)	12.492(2)
C1-C3-C4-C4^{ii}	-62(1) (***g***)	-62(1) (***g***)
C3-C4-C4^{ii}-C3^{ii}	180 (***t***)	180.0 ***(t)***
C4-C4^{ii}-C3^{ii}-C1^{ii}	62(1) (**g**)	62(1) (***g***)
Fe1···Fe1^{iii} [1-11]** (***ttt***)	13.856(1)	13.742(1)
C41-C43-C44-C44^{iii}	-179.9(9) (***t***)	173(1)(***t***)
C43-C44-C44^{iii}-C43^{iii}	180 (***t***)	180 (***t***)
Fe1···Fe1^{iv} [1-11]** (***gtg***)	12.570(1)	12.467(1)
C11-C13-C14-C14^{iv}	76(2) (***g***)	86(2) (***g***)
C13-C14-C14^{iv}-C13^{iv}	180 (***t***)	180 (***t***)
C14-C14^{iv}-C13^{iv}-C11^{iv}	-80(2) (***g***)	-86(2) (***g***)
Fe1···Fe1^{v} [200]*** (***gtg***)	12.633(1)	12.503(1)
C31-C33-C34-C54^{v}	-64(7) (***g***)	-63.7(7) (***g***)
C33-C34-C54^{v}-C53^{v}	-177.8(5) (***t***)	-177.7(5) (***t***)
C34-C54^{v}-C53^{v}-C51^{v}	55.5(7) (***g***)	55.3(8) (***g***)

Symmetry operations: ^{i}2-x, 1-y, 1-z; ^{ii} 3–x, -y, -z; ^{iii} 3-x, -y,1 -z; ^{iv} 2-x, 1-y, -z; ^{v}-1+x, y, z.

*Corresponds to [-110] bridging direction in HT structures.

**Corresponds to [10-1] bridging direction in HT structures, torsion angles are given only for one site.

***Corresponds to [001] bridging direction in HT structures.

Table S5. Selected Fe-N distances (Å), torsion angles (º) and Fe···Fe interatomic distances (Å) for: HT1(LS) at 80 K (rapid cooling) and HT1(HS) at 150 K (heating) in **1**.

	80 K (rapid cooling) HT1(LS)	**150 K (heating after rapid cooling) HT1(HS)**
Fe-N1a	2.011(2)	2.186(4)
Fe-N1b	2.001(2)	2.180(4)
Fe-N1c	2.002(2)	2.177(4)
Fe1···Fe1^{i} [-110] (***ttt***)	13.552(1)	13.769(2)
C1c-C3c-C4c-C4c^{ii}	-179.5(4)(***t***)	179.6(8) (***t***)
C3c-C4c-C4c^{ii}-C3c^{ii}	180 (***t***)	180 (***t***)
Fe1···Fe1^{iii} [10-1] (***tgt***)	13.637(1)	13.936(1)
C1b-C3b-C4b-C5b	179.4(3) (***t***)	177(1) (***t***)
C3b-C4b-C5b^{iv}-C3b^{iv}	-75.0(5) (***g***)	-87(2) (***g***)
C4b-C5b-C3b^{iv}-C1b^{iv}	178.4(3) (***t***)	-172(2) (***t***)
Fe1···Fe1^{v} [001] (***gtg***)	12.289(1)	12.391(1)
C1a-C3a-C4a-C4a^{vi}	-64.2(4) (***g***)	-65.1(8) (***g***)
C3a-C4a-C4a^{vi}-C3a^{vi}	180 (***t***)	180 (***t***)

Symmetry operations: ^{i} 1+x, -1+y, z; ^{ii} 2-x, -y, 1-z; ^{iii} -1+x, y, 1+z; ^{iv} –x, 1-y, 2-z; ^{v} x, y, -1+z; ^{vi} 1-x, 1-y, -z

Table S6. Selected Fe-N distances (Å), torsion angles (º) and Fe···Fe interatomic distances (Å) for: HT2(HS) at 170 K (heating) and HT2(LS) at 80 K (cooling) in **1** (average structure).

	170 K (heating from 150 K) HT2(HS)	**80 K (cooling from 170 K) HT2(LS)**
Fe-N1a	2.190(3)	2.004(3)
Fe-N1b	2.191(3)	2.001(3)
Fe-N1c	2.197(3)	2.010(3)
Fe1···Fe1^{i} [-110] (***ttt***)	13.795(1)	13.531(1)
C1c-C3c-C4c-C4c^{ii}	179.5(6) (***t***)	-179.4(6) (***t***)
C3c-C4c-C4c^{ii}-C3c^{ii}	180 (***t***)	180 (***t***)
Fe1···Fe1^{iii} [10-1] (***tgt***)	13.952(1)	13.592(1)
C1b-C3b-C4b-C5b	175.5(8) (***t***)	-179.4(6) (***t***)
C3b-C4b-C5b^{iv}-C3b^{iv}	-84(1) (***g***)	-81.9(9) (***g***)
C4b-C5b-C3b^{iv}-C1b^{iv}	-177(1) (***t***)	178.3(6) (***t***)
Fe1···Fe1^{v} [001] (***gtg***)	12.385(1)	12.132(1)
C1a-C3a-C4a-C4a^{vi}	-62.6(6) (***g***)	-63.4(6) (***g***)
C3a-C4a-C4a^{vi}-C3a^{vi}	180 (***t***)	180 (***t***)

Symmetry operations: ^{i} 1+x, -1+y, z; ^{ii} 2-x, -y, 1-z; ^{iii} -1+x, y, 1+z; ^{iv} –x, 1-y, 2-z; ^{v} x, y, -1+z; ^{vi} 1-x, 1-y, -z

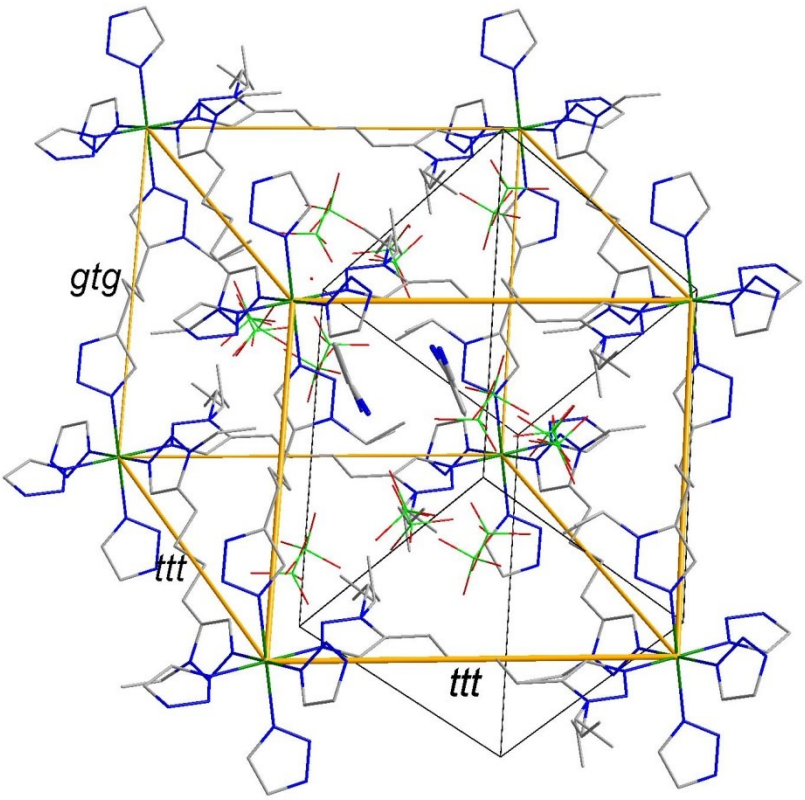

a)

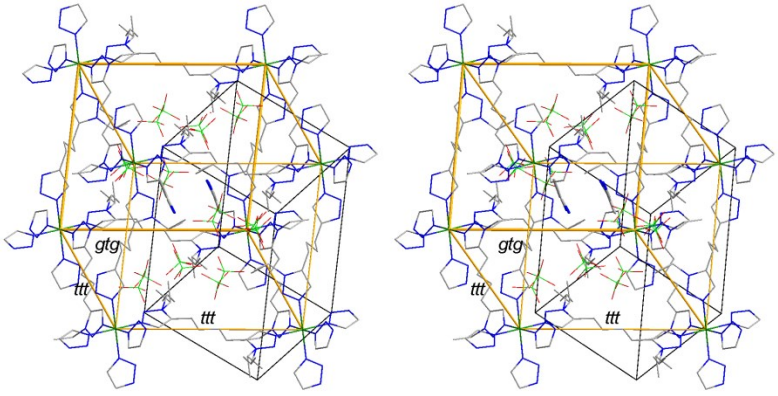

b)

Figure S1. Perspective view (a) and 3D stereoview (b) of three-dimensional network in **1** at 295 K (HT(HS) structure). Hydrogen atoms were omitted for clarity. The orange lines were added in order to track iron···iron connectivity.

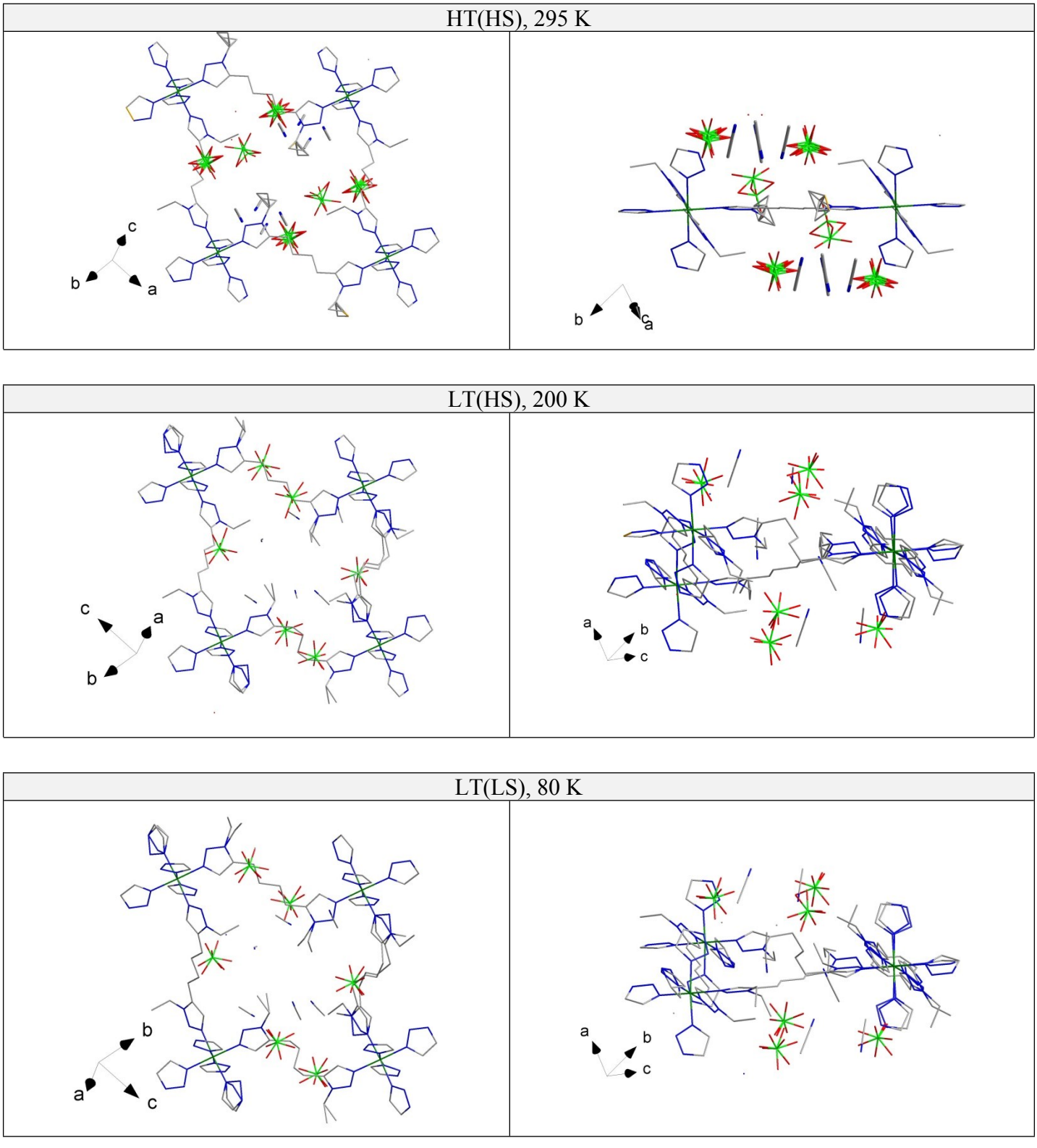

Figure S2. Comparison of the layers in **1** in: HT(HS) at 295 K, LT(HS) at 200 K, LT(LS) at 80 K showing change of conformation of ligands and vanishing of common plane created by bridged iron(II) ions (right column).

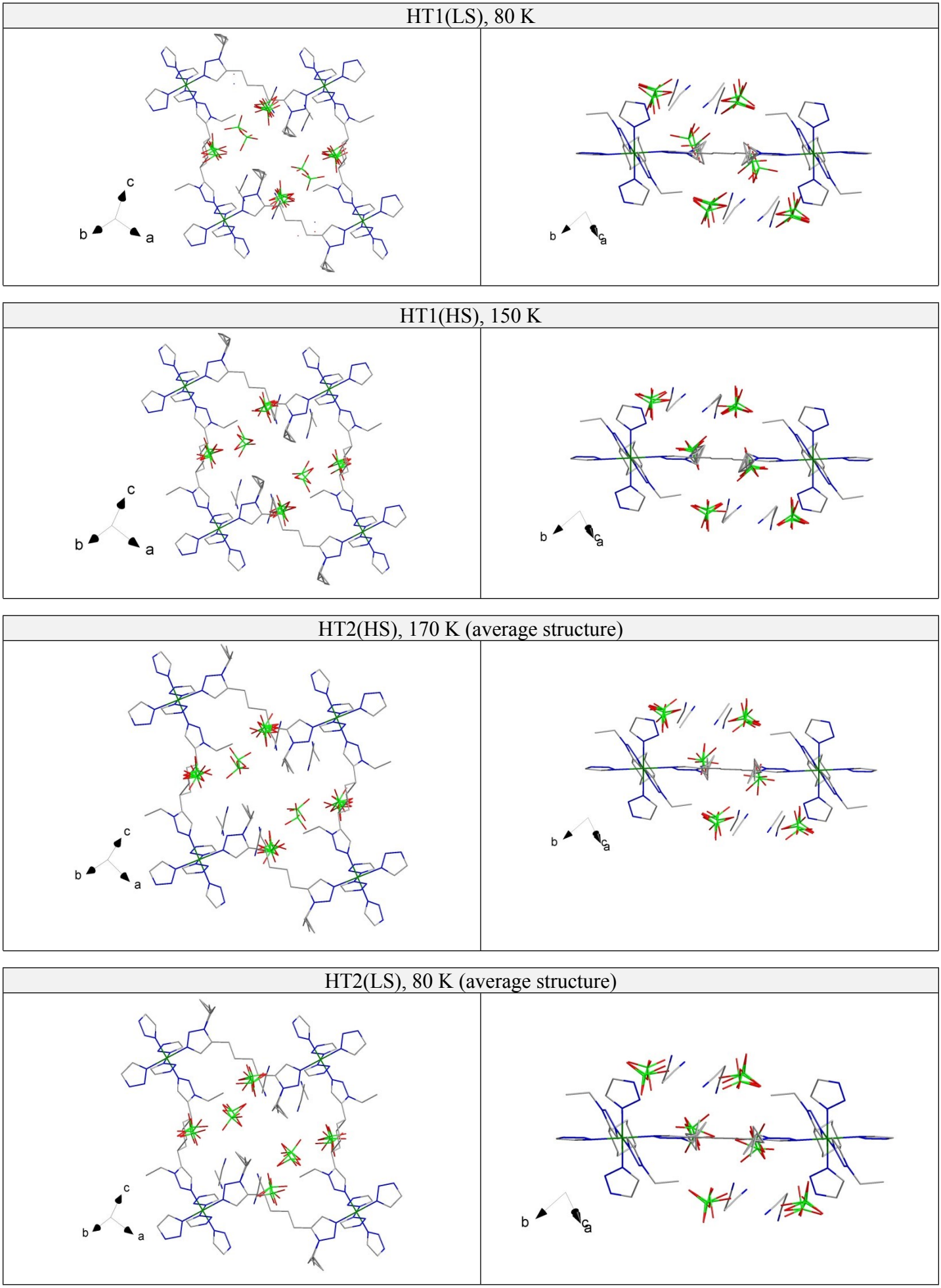

Figure S2 continued. Comparison of the layers in **1** in: HT1(LS) at 80 K, HT1(HS) at 150 K, HT2(HS) at 170 K, HT2(LS) at 80 K.

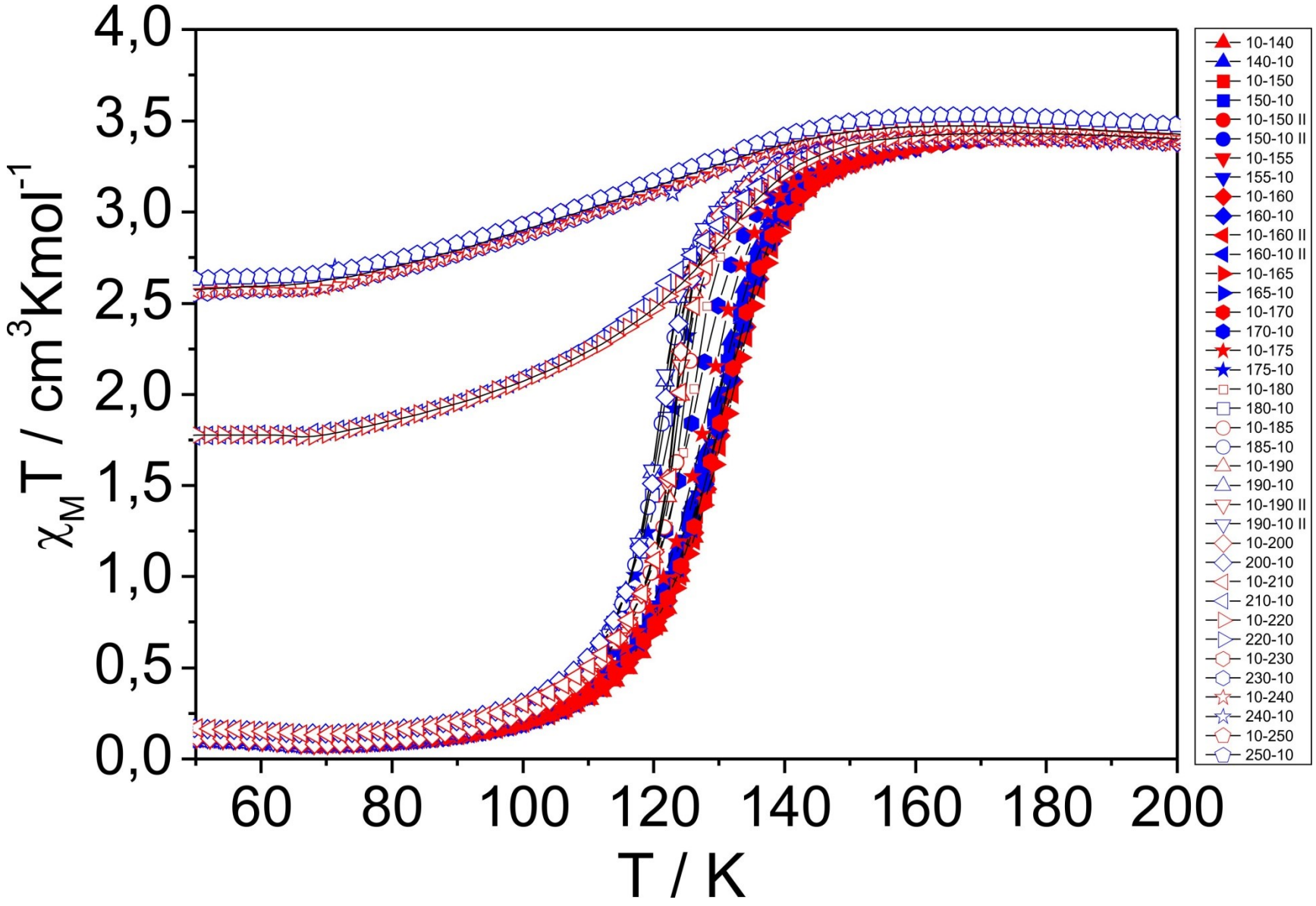

Figure S3. $\chi_M T$ vs. T dependencies obtained for consecutive heating/cooling cycles of rapidly cooled sample of **1** together with full experimental protocol placed in the frame on the right side (II denotes additional cycle (cooling/heating) in the same temperature range carried out after completion the first one). After finishing cooling/heating cycle in the given temperature range, temperature was elevated at 5 or 10 K and next cycle cooling/heating was carried out.

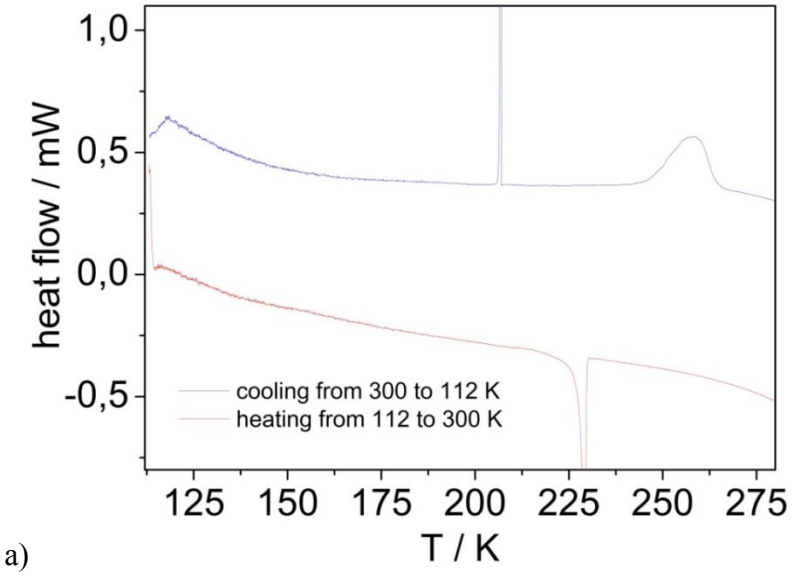

a)

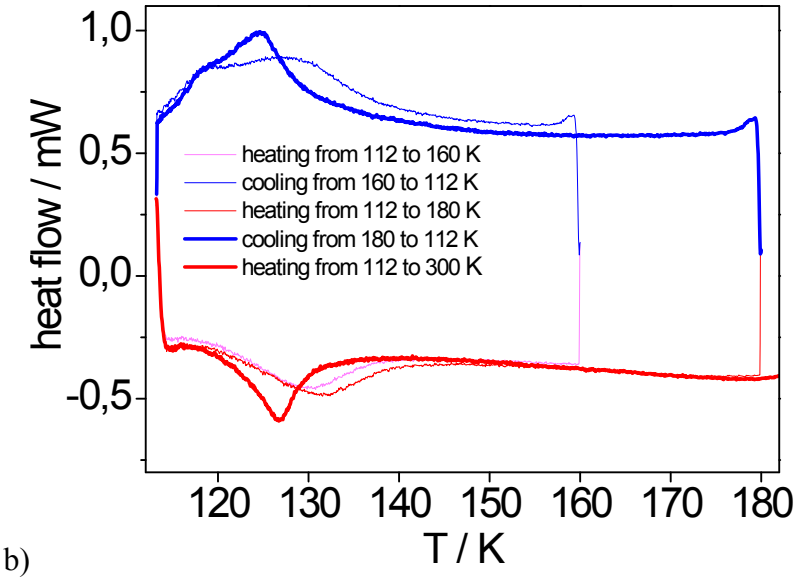

b)

Figure S4. DSC curve for **1** (wetted with acetonitrile) recoded at 2 K/min shows presence of exothermic peak during heating and absence of the one during heating (a) and measurements recorded after initial rapid cooling of sample at 112 K which was followed then by consequtive heating/coolinbg cycles recorded at 2 K/min showing a shift of peaks to lower temperatures after reaching 180 K which remains in agreement with results of magnetic and single crystal X-ray diffraction studies(b). The peaks on picture (a) around 210K (cooling) and 230 K (heating) result from presence of acetonitrile. Below 120 K the apparatus loses control of cooling velocity (2 K/min) which is visible as change of line slope.

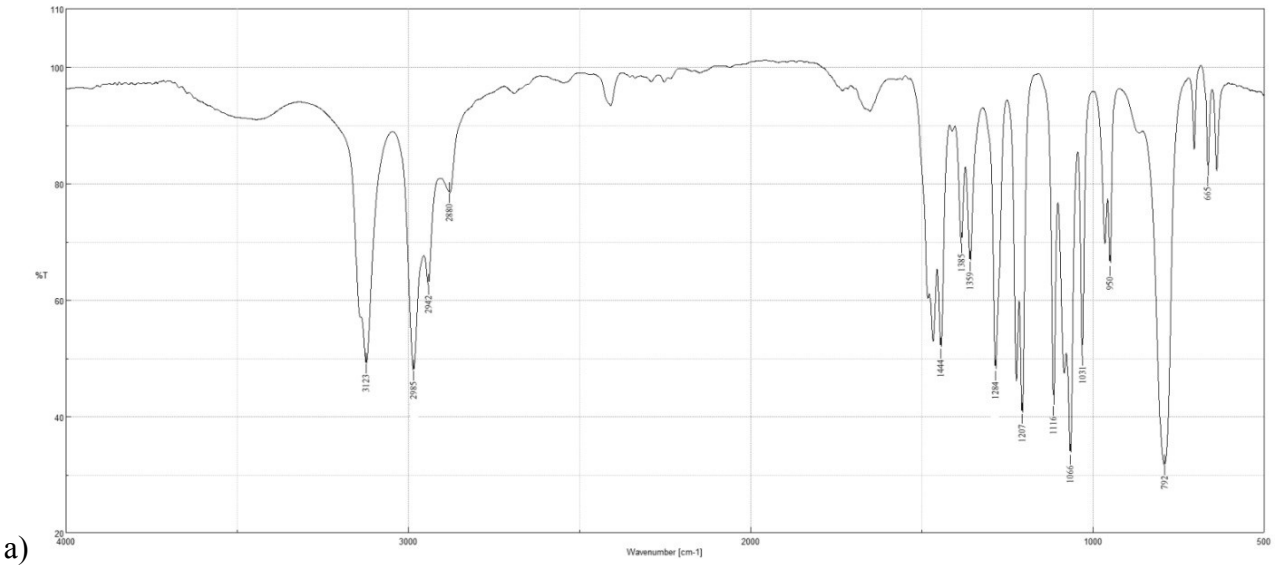

a)

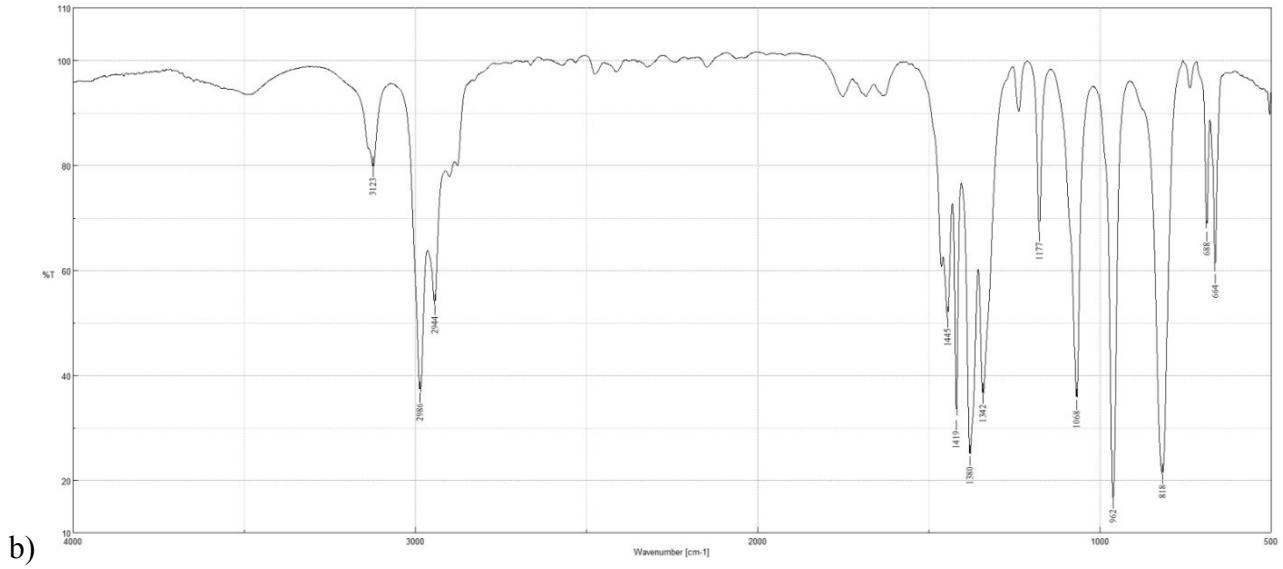

b)

Figure S5. FTIR spectra (film) for **1etr** (a), **2etr** (b).

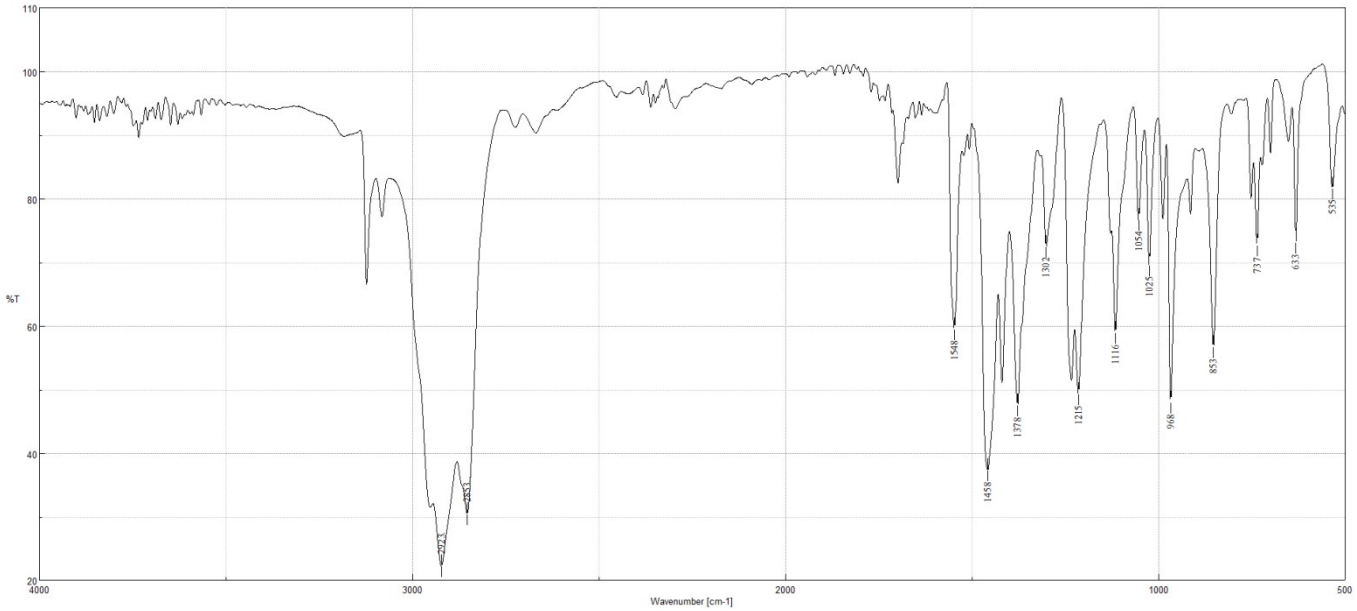

Figure S6. IR spectrum (nujol mull) for **bbtre**.

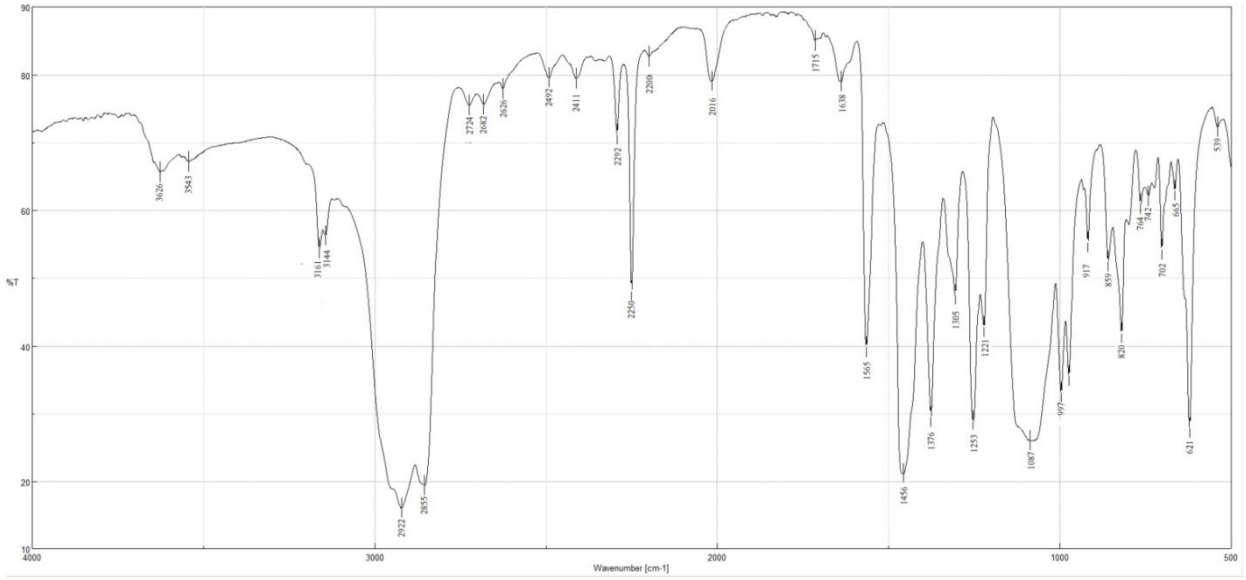

Figure S7. FTIR spectrum (nujol mull) for **1**.